Available online at www.sciencedirect.com

SciVerse ScienceDirect

Ceramics International 39 (2013) 153–157

CERAMICS INTERNATIONAL

www.elsevier.com/locate/ceramint

Rapid fabrication of diamond-structured ceramic photonic crystals with graded dielectric constant and its controllable stop band properties

Qingxuan Liang*, Dichen Li, Gai Yang

State Key Laboratory of Manufacturing Systems Engineering, Xi'an Jiaotong University, Xi'an 710049, China

Received 17 May 2012; received in revised form 1 June 2012; accepted 1 June 2012
Available online 15 June 2012

Abstract

Three-dimensional (3D) inverse diamond-structured ceramic photonic crystals (PCs) were fabricated by stereolithography (SL) and gel-casting process using alumina slurry. The gradually varied solid loading in volume and its controllable stop band properties were studied in the PCs. It was found that, with the decrease ratio of the solid loading increasing, the stop band width decreased and the center frequency of the stop band shifted to the higher frequency range. Several PCs containing two graded solid loading of alumina simultaneously along the Γ–X ⟨100⟩ direction were also fabricated in the same process to investigate their complex stop band properties. Compared with the perfect PC, the stop band width of the graded solid loading PCs increased remarkably with the decrease ratio of the solid loading increasing when the electromagnetic wave transmits along the Γ–X ⟨100⟩ direction. When the decrease ratio reached to 10%, the stop band width reached 126.5% of that of the perfect PC, which agreed well with the Finite Integration Technique (FIT).

Keywords: A. Shaping; C. Electrical properties; Photonic crystals; Stereolithography

1. Introduction

Three-dimensional (3D) photonic crystals (PCs), structures with periodic variation of dielectric constant that can manipulate the propagation of the electromagnetic wave in all directions, have attracted considerable attentions in recent years for their wide potential applications [1–6]. For some applications of PCs, a wider stop band width is favorable so that wave control in a wide range can be realized. The stop band can be controlled by varying the structure, filling ratio, and dielectric constant of the lattice materials [7,8]. The PCs of various 3D structures have been widely investigated through theoretical calculation and experimental evaluation. Among the various structures, diamond structure is one of the most attractive class of structures, which consists of two interpenetrating face centered cubic Bravais lattices. It is difficult, however, to form 3D diamond structures because the lattice stacking is difficult to achieve compared with simple face-centered cubic or woodpile structures [9,10]. Most of the research efforts on the diamond structure are concentrated on the structural parameters modifications and varying the dielectric constant in order to get the wider stop band width [11–13]. However, little work has been done on broadening the stop band width by gradient dielectric constant induced by the variation of solid loading of ceramic powder in the slurry in the fabrication process of PC.

Various processes have been used for fabricating diamond-structured PCs [14–17]. But these are less suitable for the PCs with multi solid loading ceramics coupling because achieving multi solid loading ceramics coupling structures has been a technological challenge up to now, even through the PCs in the microwave range are regarded to be easily fabricated. Gel-casting is an attractive ceramic forming process, which can produce high quality complex-shaped ceramic green bodies [18–21]. In such a process, a high solid loading slurry consisting of ceramic power, solvent and organic binder is first required. After the slurry is cast into a mold, the organic binder creates a macromolecular network to hold the ceramic particles together. The aqueous ceramic slurry has low viscosity

*Corresponding author. Tel.: +86 29 82665987; fax: +86 29 82660114.
E-mail address: liangqx728@gmail.com (Q. Liang).

0272-8842/$36.00
http://dx.doi.org/10.1016/j.ceramint.2012.06.003

and fill up mold cavities with ease, the complexity of shape attained by gel-casting is limited only by the ability of mold design. Stereolithography (SL) is a typical rapid prototyping process and has the capability of rapidly fabricating any complex-shaped resin prototypes which have high forming accuracy, good rigidity and fine surface quality. So we proposed a rapid prototyping method by combining SL with gel-casting for the easy fabrication of the different solid loading ceramics coupling PCs.

In the present work, diamond-structured PCs composed of air spheres using alumina slurries with the same structure parameters but with different solid loading in volume were firstly fabricated by SL and gel-casting process, and the influence of the gradually varied solid loading on the stop band property was experimentally investigated. The diamond-structured PCs containing two different solid loading in volume of alumina simultaneously were then fabricated in the same process to investigate the changes of stop band properties along the combined direction $\langle 100 \rangle$ of the PCs. This method resulted in an interface between the different solid loading alumina parts which forms a gradient dielectric constant distribution in the PCs. As a result, the structure would have a gradually varying stop band when either of solid loadings of alumina was varied. Experimental result was compared with the simulation result by the FIT (CST MWS2010, Computer Simulation Technology, Darmstadt, Germany).

2. Experimental procedure

In this research, the SL and gel-casting process was employed to fabricate the diamond-structured PCs. The diamond-structured PC models were designed based on the FIT, and the corresponding PCs molds were fabricated using a stereolithographic machine (Product SPS-450B, Hengtong Co. Ltd, Shaanxi, China). This SL system formed a three-dimensional object layer by layer by scanning an ultraviolet laser of 355 nm wavelength over a liquid photopolymer epoxy resin. The diameter of the beam spot was 100 μm with a scanning speed of 90 mm/s in operation and a single layer thickness of 100 μm. The dimensional accuracy of the structure obtained was within 0.1%.

In the gel-casting process, the casting slurries with Al_2O_3 powder were prepared firstly. In this process, a premixed solution was prepared by dissolving organic monomer (CH_3CONH_2, AM) and cross-linking agent ($C_7H_{10}N_2O_2$, MBAM) in appropriate amount of deionized water. After adding an appropriate amount of sodium polyacrylate (25% of solid powder in mass) to the premixed solution, Al_2O_3 powder was dispersed into the premixed solution progressively. Alumina ceramic slurries with high solid loadings (50 vol%, 52.5 vol%, 55 vol%, 57.5 vol%, and 60 vol%) were prepared after milling for 3 h. After adding the initiator ammonium persulfate and catalyst ($C_6H_{16}N_2$, TEMED) into the ceramic slurries, the ceramic slurries were stirred in vacuum for 5 min to degas and then smoothly poured into their molds. Then the ceramic slurries were polymerized in situ. The fabrication process of the PC with the solid loading of 60 vol% and 50 vol% simultaneously is shown in Fig. 1. Firstly, the alumina slurry (60 vol%) was poured into the mold from the casting mouth and the connectivity port maintained the alumina slurry at half the height of the PC mold. Secondly, the casting mouth and the connectivity port was blocked using plasticine. Finally, alumina slurry (50 vol%) was rapidly poured into the mold from the top when the alumina slurry (60 vol%) was being polymerized. The other PCs with two different solid loadings of alumina powder were also fabricated in the same process. The parts could be partially unmolded and then were dried using the freeze drying oven for 36 h under a vacuum degree of 3 Pa (Product DTY-1SL, Vacuum Freeze Dryer, Detianyou Technology Co., Beijing, China). In the end, the samples were sintered at 1550 °C for 2 h. The resin prototype was burned out and ceramic PCs of high quality were obtained.

The lattice constant a was 7 mm and the air sphere radius r was chosen to be $0.28a$. The stop band was expected to occur in the frequency region of 18–40 GHz according to the simulation results by the FIT. The dimension of the diamond structure was 49 mm × 42 mm × 42 mm. The solid loading of the perfect alumina PC was set as 60 vol%. The solid loading was then decreased to 2.5 vol%, 5 vol%, 7.5 vol%, and 10 vol% based on the perfect PC. The decrease ratio is defined as difference between the perfect PC's solid loading and that of the decreased PC, which means that if the solid loading is decreased 2.5 vol%, the decrease ratio will be 2.5%. To investigate the stop band properties of the PCs with graded dielectric constant, several coupling PCs by combining the perfect PC with the decreased PCs that the decrease ratio is 2.5%, 5%, 7.5%, and 10% respectively were also fabricated.

The microstructure was observed using scanning electron microscopy (SEM) (S-3000N, Hitachi, Tokyo, Japan). Microfocus computed tomography (Micro-CT) (Y. Cheetah, YXLON International GmbH, Hamburg, Germany) was used to evaluate structural array of the alumina PCs.

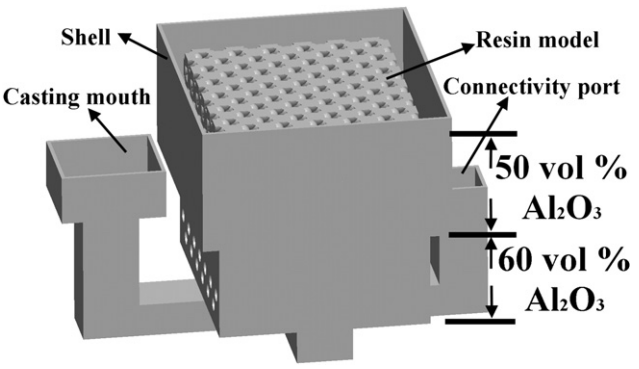

Fig. 1. The fabrication process of the photonic crystal with the solid loading of 60 vol% and 50 vol% simultaneously by stereolithography and gel-casting process.

The transmission properties of the PCs were measured in the frequency of 18–40 GHz using a free space measurement system with a network analyzer (Agilent E8363B, Agilent Technologies Inc., Palo Alto, CA).

3. Results and discussion

Fig. 2 shows the SEM photos of the alumina PCs with the decrease ratio of the solid loading of 10% (a), 5% (b) and the perfect PC (c) sintered at 1550 °C for 2 h. The images reveal the influence of the solid loading of the alumina powder on the ceramic microstructure. Homogeneous dense microstructure can be observed and some micropores exit in the three photos. Comparing the three SEM photos, it can be found that, with the decrease ratio of the solid loading decreasing, the microstructure become denser and pores become fewer. This results in higher dielectric constant of the alumina PCs.

Fig. 3 shows 3D reconstruction images of the alumina PC with graded dielectric constant (the perfect PC and that of the decrease ratio of 10% simultaneously) using the Micro-CT analysis. It can be observed that the PC has no crack and is uniform well after sintering in Fig. 3(a). In Fig. 3(b), the image reveals clearly that a periodic structure was arranged and the dielectric parts were well connected together to build a 3D structure. Therefore the SL and gel-casting process was proven to be a suitable technique for diamond-structured PC.

Fig. 4 shows the relationship between the stop band properties and the decrease ratio of the solid loading of alumina powder in the Γ–X ⟨100⟩ direction of the PCs. The closed circle solid line and the square solid line show the measurement results of the center frequency and the stop band width respectively. In all cases, the structure parameters were kept unchanged and the solid loading was varied to change the dielectric constant. It was found that, with the decrease ratio increasing, the measured stop band width decreased gradually and the center frequency of the stop band shifted to a higher frequency. When the decrease ratio of the solid loading reached 10%, the stop band width changed from 6.8 GHz to 4.9 GHz and the center frequency increased from 29.4 GHz to 32.2 GHz. The results indicated that the change of the solid loading in volume of ceramic powder had an obvious influence on the stop band properties of PCs.

Fig. 5 shows the relationship between the measurement results of the stop band width and the decrease ratio along the Γ–X⟨100⟩ direction of the PCs with graded dielectric constant. The dimension of the PCs of gradient dielectric constant was also 49 mm × 42 mm × 42 mm. This included the perfect alumina PC (60 vol%) with the dimension of 49 mm × 42 mm × 21 mm and the decreased alumina PC (the decrease ratio was 2.5%, 5%, 7.5%, 10%) with the

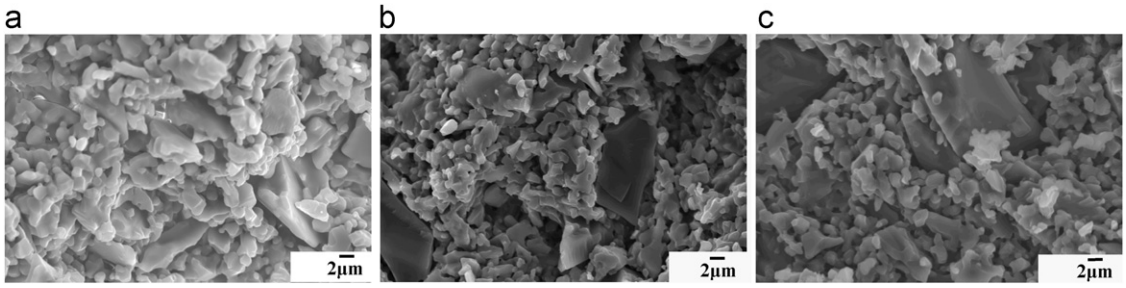

Fig. 2. The SEM photos of the alumina photonic crystals with the decrease ratio of solid loading of 10% (a), 5% (b) and the perfect photonic crystal (c) sintered at 1550 °C for 2 h.

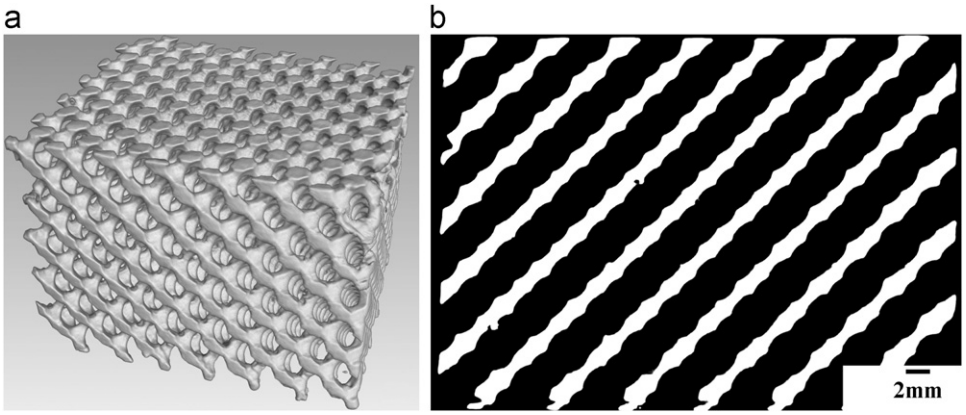

Fig. 3. Three-dimensional reconstruction images of the alumina photonic crystal with graded dielectric constant (the perfect photonic crystal and that of the decrease ratio of 10% simultaneously) using Micro-CT analysis: (a) three-dimensional reconstruction image. and (b) top view of the cross-sectional reconstruction image.

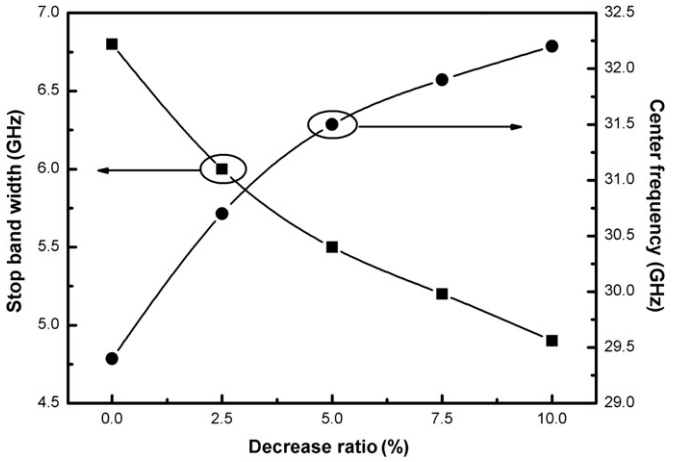

Fig. 4. The relationship between the stop band properties and the decrease ratio of the solid loading of alumina powder in the Γ–X ⟨100⟩ direction of the photonic crystals.

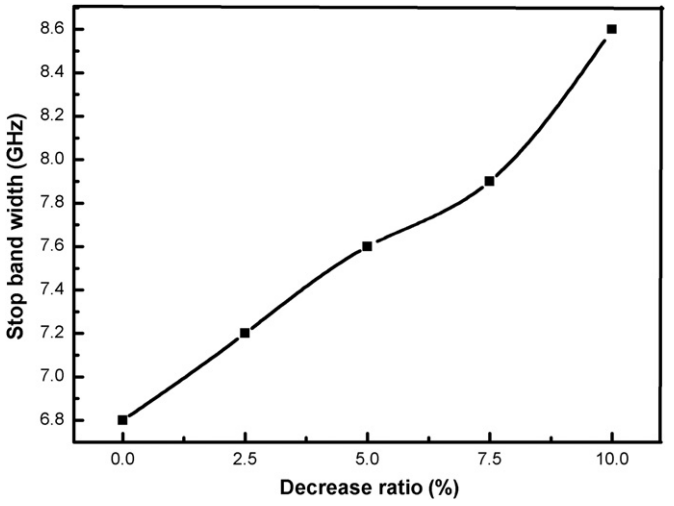

Fig. 5. The relationship between the measurement results of the stop band width and the decrease ratio along the Γ–X ⟨100⟩ direction of the photonic crystals with graded dielectric constant.

same dimension. It was found that, with the decrease ratio of the solid loading of the graded solid loading PCs increasing, the stop band width increased gradually, and that it became 126.5% of that of the perfect alumina PC when the decrease ratio was 10%. This result can be attributed to the variation of the center frequency of the decreased structures. As shown in Fig. 4, the center frequency of the stop band increased with the decrease ratio of the solid loading Al_2O_3 powder increasing. Because the PCs of gradient dielectric constant was constituted by uniting two separate PCs with different solid loadings in volume together, the stop band width of the PCs of gradient dielectric constant would increase due to the overlapping of the stop bands of each PC. Furthermore, the dielectric contrast of the interface of the two PCs was not continuous therefore the stop bands were formed by Bragg scattering. The sudden variation of the dielectric contrast on the interface strengthened the Bragg scattering and increased the bandwidth finally.

Fig. 6 shows the simulation and measurement results of the PC with graded dielectric constant containing the perfect alumina PCs and that with the decrease ratio of 10% simultaneously along the Γ–X ⟨100⟩ direction. The measurement results demonstrate an electromagnetic stop band between 26.4 GHz and 35 GHz. The stop band width is 8.6 GHz and this is 1.8 GHz wider than that of the perfect alumina PC (60 vol%). The maximum attenuation attained is −55.3 dB. Comparing the experimental results with the simulation results obtained by the FIT, there was a good agreement between the two. The result can be attributed to the graded dielectric constant in the PC.

4. Conclusion

In summary, the diamondstructured PCs with gradually varied solid loading in volume of alumina powder were fabricated successfully by combining the SL with gel-casting process and its controllable stop band properties were investigated. It was found that the stop band width decreased and the center frequency of the stop band shifted to the higher frequency range as the decrease ratio of the solid loadings increased. Several PCs containing two solid loading in volume of alumina simultaneously along the Γ–X ⟨100⟩ direction were also fabricated in the same process to investigate their complex stop band properties. Compared with the perfect PC, the stop band width of the graded solid loading PCs increased remarkably with the decrease ratio of the solid loading increasing when the electromagnetic wave transmits along the Γ–X ⟨100⟩ direction. When the solid loading decreased to 10% of the perfect PC, the stop band width reached 126.5% of that of the perfect PC, which agreed well with the FIT.

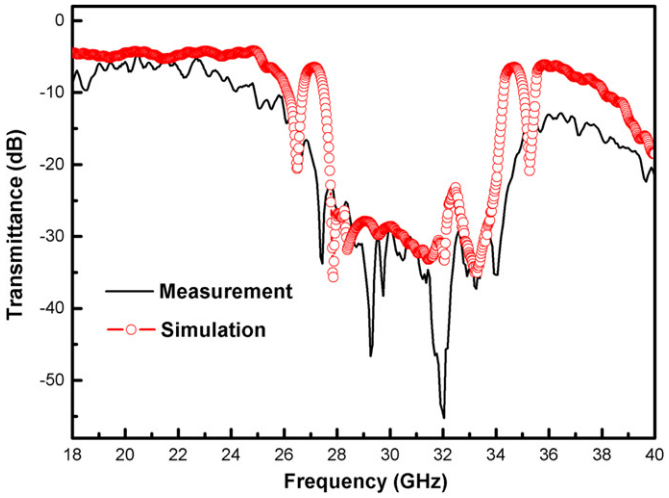

Fig. 6. The simulation and measurement results of the photonic crystal with graded dielectric constant containing the perfect alumina photonic crystal and that with the decrease ratio of 10% simultaneously along the Γ–X ⟨100⟩ direction.

Acknowledgments

This work was supported by the Key NSFC Project of China under Grant no 50835007, Ph.D. Programs Foundation of Ministry of Education of China under Grant 20090201110038.

References

[1] K. Ho, C. Chan, C. Soukoulis, Existence of a photonic gap in periodic dielectric structures, Physical Review Letters 65 (25) (1990) 3152–3155.
[2] M. Maldovan, E.L. Thomas, Diamond-structured photonic crystals, Nature Materials 3 (9) (2004) 593–600.
[3] P.V. Parimi, W.T. Lu, P. Vodo, S. Sridhar, Photonic crystals: imaging by flat lens using negative refraction, Nature 426 (6965) (2003) 404.
[4] D. Armani, T. Kippenberg, S. Spillane, K. Vahala, Ultra-high-Q toroid microcavity on a chip, Nature 421 (6926) (2003) 925–928.
[5] N. Delhote, D. Baillargeat, S. Verdeyme, M. Thevenot, C. Delage, C. Chaput, Large experimental bandpass waveguide in 3D EBG woodpile manufactured by layer-by-layer ceramic stereolithography, in: Proceedings of the IEEE MTT-S International Microwave Symposium, 2007, pp. 1431–1434.
[6] J. Zimmermann, M. Kamp, A. Forchel, R. März, Photonic crystal waveguide directional couplers as wavelength selective optical filters, Optics Communications 230 (4) (2004) 387–392.
[7] W. Dai, H. Wang, D. Zhou, Z. Shen, Y. Li, D. Li, The ultra-wide band gap property induced by lattice period gradually changing in three-dimensional photonic crystals, Journal of the American Ceramic Society 93 (12) (2010) 3980–3982.
[8] X. Lu, Y. Lee, S. Yang, Y. Hao, R. Ubic, J.R.G. Evans, C.G. Parini, Fabrication of millimeter-wave electromagnetic bandgap crystals using microwave dielectric powders, Journal of the American Ceramic Society 92 (2) (2009) 371–378.
[9] E. Yablonovitch, T. Gmitter, Photonic band structure: the face-centered-cubic case, Physical Review Letters 63 (18) (1989) 1950–1953.
[10] X. Lu, Y. Lee, S. Yang, Y. Hao, R. Ubic, J.R.G. Evans, C.G. Parini, Fabrication of electromagnetic crystals by extrusion freeforming, Metamaterials 2 (1) (2008) 36–44.
[11] S. Kanehira, S. Kirihara, Y. Miyamoto, K. Sakoda, M.W. Takeda, Band gap modification of diamond photonic crystals by changing the volume fraction of the dielectric lattice, Journal of the American Ceramic Society 86 (10) (2003) 1691–1694.
[12] S. Kirihara, M. Takeda, K. Sakoda, Y. Miyamoto, Electromagnetic wave control of ceramic/resin photonic crystals with diamond structure, Science and Technology of Advanced Materials 5 (1–2) (2004) 225–230.
[13] Q. Liang, D. Li, G. Yang, Controllable bandgap properties induced by the air sphere radius variation in diamond-structured ceramic photonic crystals, Journal of the American Ceramic Society 94 (12) (2011) 4134–4137.
[14] J.W. Galusha, M.R. Jorgensen, M.H. Bartl, Diamond-structured titania photonic-bandgap crystals from biological templates, Advanced Materials 22 (1) (2010) 107–110.
[15] S. Kirihara, Y. Miyamoto, K. Takenaga, M.W. Takeda, K. Kajiyama, Fabrication of electromagnetic crystals with a complete diamond structure by stereolithography, Solid State Communications 121 (8) (2002) 435–439.
[16] G.V. Prakash, R. Singh, A. Kumar, R.K. Mishra, Fabrication and characterisation of CdSe photonic structures from self-assembled templates, Materials Letters 60 (13–14) (2006) 1744–1747.
[17] K. Takagi, A. Kawasaki, Fabrication of three-dimensional terahertz photonic crystals with diamond structure by particle manipulation assembly, Applied Physics Letters 94 (2009) 021110.
[18] X. Xu, Z. Wen, J. Lin, N. Li, X. Wu, An aqueous gel-casting process for γ-$LiAlO_2$ ceramics, Ceramics International 36 (1) (2010) 187–191.
[19] M. Dong, X. Mao, Z. Zhang, Q. Liu, Gelcasting of SiC using epoxy resin as gel former, Ceramics International 35 (4) (2009) 1363–1366.
[20] D. Kong, H. Yang, S. Wei, D. Li, J. Wang, Gel-casting without de-airing process using silica sol as a binder, Ceramics International 33 (2) (2007) 133–139.
[21] J.-M. Tulliani, C. Bartuli, E. Bemporad, V. Naglieri, M. Sebastiani, Preparation and mechanical characterization of dense and porous zirconia produced by gel casting with gelatin as a gelling agent, Ceramics International 35 (6) (2009) 2481–2491.